Identification of a Region of the Ileal-Type Sodium/Bile Acid Cotransporter Interacting with a Competitive Bile Acid Transport Inhibitor

S. Hallén,[‡,§] A. Björquist,[§] A. M. Östlund-Lindqvist,[§] and G. Sachs*[,‡]

UCLA and the Wadsworth Veterans Administration Hospital, Los Angeles, California 90073, and AstraZeneca R&D, Mölndal, Sweden

Received August 19, 2002; Revised Manuscript Received September 30, 2002

ABSTRACT: Drug intervention that prevents reabsorption of circulating bile acids by the apical (ileal) sodium/bile acid cotransporter (ASBT) may be a promising new therapy for lowering of plasma cholesterol. 2164U90 is a benzothiazepine-based competitive inhibitor of bile acid transport with K_i values of ∼10 and 0.068 μM for the homologous human and mouse apical transporters, respectively. Hybrid human−mouse and mouse−human transporters were engineered to identify regions involved in this 150-fold difference in the inhibition constant for 2164U90. A mouse−human chimera with only the most C-terminal hydrophobic domain and the C-terminus of the transporter originating from the human variant was found to have a sensitivity to 2164U90 inhibition similar to that of the human transporter. Conversely, a human−mouse hybrid transporter encompassing the same C-terminal region from the mouse sequence but now inserted into the human sequence demonstrated the greater inhibition seen with the mouse wild type ASBT. Amino acid substitutions, individually or in combinations, of six candidate nonconserved residues between mouse and human transporters in this C-terminal domain showed replacements of Thr294 by Ser and Val295 by Ile to be responsible for the difference in the sensitivity toward 2164U90 seen between the species. The hamster apical SBAT encompassing Ser/Ile in these positions shared the lower sensitivity to 2164U90, as seen with the human ASBT, even though it is identical to the mouse SBAT in the remaining four positions of this region. In addition, the rat ASBT which is identical to the mouse ASBT in this domain also had the high sensitivity to 2164U90 inhibition found for the mouse ASBT. Methanethiosulfonates (MTS) are known to inactivate the sodium/bile acid transporters through alkylation of a cysteine in the most C-terminal hydrophobic domain (*1*). Inactivation of the human ASBT due to MTS modification of cysteine 270 was shown to be largely abolished when the transporter was preincubated with 2164U90, suggesting that the binding of this benzothiazepine is in the vicinity of position 270. Thus, the domain containing the two most C-terminal putative transmembrane regions of the SBATs, H8−H9, previously shown to constitute part of the binding pocket for bile acids, interacts also with the bile acid transport competitive inhibitor, 2164U90.

Bile acids are important in control of cholesterol homeostasis. Cholesterol is the precursor for bile acid synthesis in the liver, and bile acids are important detergents in solubilizing cholesterol in bile as well as in the gut. Interruption of the enterohepatic circulation of bile acids in the small intestine causes a compensatory increase in conversion of cholesterol into bile acid in the liver. Drug intervention that prevents reabsorption of bile acids by the ileal SBAT[1] is potential therapy for lowering of serum cholesterol (*2*).

Bile acids are preserved in circulation between the liver and the small intestine by a number of polytopic membrane proteins and intracellular carrier proteins. Reabsorption of bile acids from the intestinal lumen, the portal blood, the bile duct and the kidney is facilitated mainly by sodium/bile acid co-transporters (SBATs) (*3*). Two homologous SBATs are found in mammals, one type with an apical distribution in ileal/renal enterocytes and bile duct cholangiocytes and another that is trafficked to the basolateral sinusoidal membrane of hepatocytes. Apical and basolateral sodium/bile acid co-transporters have been cloned from a number of species including hamster, rat, rabbit, mouse, and human (*4*−*12*). They share ∼35% identity and have very similar hydrophobicity profiles, indicating a common SBAT core structure that has a glycosylated exoplasmic N-terminus, 7 or 9 transmembrane segments, and a cytoplasmic C-terminus (*6*, *13*−*15*). However, there are substantial differences in the range of substrates that are transported, the apical SBATs being selective for translocation of mainly the natural bile acids while the basolateral SBATs also transport a variety of organic anions. The same trend holds for SBAT inhibitors where a number of compounds selective for either

[†] This work was supported by USVA and NIH Grants DK46917, 53462, 41301, and 17294.

* Corresponding author. Address: Membrane Biology Laboratory, West Los Angeles VA Medical Center, 11301 Wilshire Blvd., Bldg. 113, Rm 324, Los Angeles, CA 90073. Tel: (310) 268-4672. Fax: (310) 312-9478. E-mail gsachs@ucla.edu.

[‡] UCLA and the Wadsworth Veterans Administration Hospital.

[§] AstraZeneca R&D.

[1] Abbreviations: SBAT, sodium bile/acid cotransporter; ASBT, apical sodium/bile acid cotransporter; TM, transmembrane; PAGE, polyacrylamide gel electrophoresis; MHBSS, modified Hanks balanced salt solution; ChCl, choline chloride; kDa, kilodalton; MTS, methanethiosulfonate; MTSET, [2-(trimethylammonium)ethyl]methanethiosulfonate; SPA, scintillation proximity assay; TCA, taurocholic acid; SNP, single nucleotide polymorphism.

10.1021/bi0205404 CCC: $22.00
Published on Web 11/19/2002

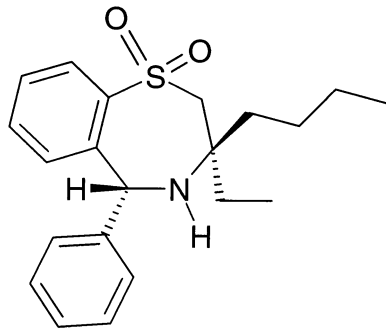

FIGURE 1: 2164U90 ((3*R*,5*R*)-3-butyl-3-ethyl-5-phenyl-2,3,4,5-tetrahydro-1,4-benzothiazepine 1,1-dioxide).

the ileal or the liver SBATs have been identified (*16*). Overall, the ileal (apical family) SBATs from different species exhibit ~73% identity (85% similarity), and they demonstrate comparable affinity for the natural substrates, bile acids and sodium, when expressed in mammalian cells (*4*, *9*, *16*, *17*).

Several types of bile acid reabsorption inhibitors have been described (*18*−*21*). A benzothiazepine compound, 2164U90 (Figure 1), has been shown to efficiently block bile acid uptake via the ileal transporter in both in vitro and in vivo models (*21*, *22*). This compound and analogous structures are competitive inhibitors of the ileal sodium/bile acid cotransporter, but no information on the site of interaction between transporter and drug has been presented. A ~150-fold difference in the K_i values for 2164U90 inhibition of the human and mouse ileal sodium/bile acid cotransporter provided an opportunity to define the region of interaction between inhibitor and protein. Chimeric constructs containing different regions of the two transporters were used along with site-directed mutagenesis and two amino acids in the mouse transporter, threonine 294 and valine 295, as compared to serine and isoleucine in the human transporter appear responsible for the 150-fold shift in the K_i of the inhibitor.

EXPERIMENTAL PROCEDURES

Reagents. 2164U90 ((3*R*,5*R*)-3-butyl-3-ethyl-5-phenyl-2,3,4,5-tetrahydro-1,4-benzothiazepine 1,1-dioxide) was synthesized at AstraZeneca, Mölndal.

Construction of Hybrid Transporters, Site-Directed Mutagenesis, and Cloning Procedures. All transporter chimeras were made by a two-step PCR method fusing the human and mouse ASBTs at desirable positions encompassing high homology between the transporters. Hybrid transporters starting with the mouse ASBT sequence and ending with human ASBT sequence were linked by overlapping PCR primers at the following positions (mouse sequence underlined): MH C1, IKRPWG; MH C2, IDGDMD; MH C3, KAKIIL; MH C4, WYRCRT. The corresponding human−mouse chimeras were fused at the following: HM C3, KAKIIL; and HM C4, WYRCRT (human sequence underlined). Site-directed mutations in the apical mouse sodium/bile acid co-transporters were introduced by the use of the QuikChange kit from Stratagene. Mutant oligonucleotides for the various substitutions were constructed using the Primer Select software and purchased from Gibco Life Technologies. cDNA for the human, mouse, rat, and hamster SBATs was a kind gift of Dr Paul Dawson, Wake Forest University, and the individual SBATs were cloned into the pcDNA3 vector from Invitrogene. Samples of 1−2 μL of the *Dna*I digested PCR products following the QuikChange protocol were transformed into JM109 by electroporation using Bio-Rad's electropulser at 1.5 kV, 800 ohms, and 25 μF. Plasmids were purified using anion exchange columns (Qiagen, Chatsworth, CA), and all mutations were verified by dideoxy sequencing.

Expression in HEK293 Cells. HEK293 cells grown to 70−80% confluence in Dulbecco's Modified Eagle Medium (high glucose, supplemented with 10% fetal bovine serum, 100 units/L penicillin, 0.1 mg streptomycin/l, 2 mM L-glutamine, 0.1 mM nonessential amino acids, and 1.0 mM sodium pyruvate) was trypsinized by washing the monolayer with PBS before adding 0.05% trypsin/53 mM EDTA (Gibco Life Technologies), and single cells were recovered by centrifugation. Approximately 3×10^4 cells in 100 μL DMEM were then added to each well in a Cytostar SPA 96 w plate. After 1 day, cells were transfected with 0.075 μg DNA/well using the FuGENE6 transfection reagent from Roche Molecular Biochemicals according to the manufacturer's recommendations. On day 2−3 (24−48 h after transfection), cells were 90−100% confluent in the Cytostar-T 96 well plate, and [^{14}C]-taurocholate (NEN Life Science Products, Inc.) uptake activity was measured using a Micro-β scintillation plate reader (EG&G/Wallac) as described previously (*23*).The HEK293 cells were then lysed in a buffer containing 15% SDS, 8 M urea, 10% sucrose, 62.5 mM Tris-HCl, pH 6.8, 10 mM EDTA, and 5 mM DTT. The approximate expression levels of the transporter constructs were then determined by Western blotting of ~10 μg total cell−lysate separated on a precast 1.5 mm 10% Tris/glycine gel (Novex) and then electrotransferred to PVDF membrane (Millipore Immobilon-P, 0.22 μM). The efficiency of the transfer was verified by Coomassie staining of the membrane prior to immunoblotting. The primary antibody for detection of the apical SBATs was an affinity-purified polyclonal antibody from rabbit raised against the human ASBT C-terminal fragment, −CEPESSFYKANGGFQPDEK (QCB Inc.). The secondary antibody was a goat anti-rabbit-HRP conjugated polyclonal antibody from American Qualex. Detection was with the ECL-Plus chemiluminescence reaction from Amersham/Pharmacia.

Measurement of Kinetic Parameters for Taurocholate Transport and 2164U90 Inhibition. $K_{m,app}$ values for taurocholate uptake by the ASBTs were monitored as described previously (*1*). In short, transiently transfected HEK293 cells grown in Cytostar 96w SPA plates were incubated with 50 μL 5−40 μM of ^{14}C-taurocholate (10 Ci/mol), and the accumulation of ^{14}C was recorded real-time in a Micro-β plate reader. The instrument was set at 1 min repetitive readings, and the initial accumulation was followed for 10 min total at room temperature (10 data points). Uptake rate was defined as the slope of plotting CPM versus time. Using a similar protocol, 2164U90 inhibition was detected at 50 μM ^{14}C-taurocholate, and the amount of intracellular ^{14}C at steady-state accumulation (~60 min) was fitted to the equation

$$y = 100\%/(1 + (x/IC_{50})^s)$$

and IC_{50} curves were generated, where y is percent activity of control at x μM of 2164U90 while s represents a slope

factor. Stock solutions of 2164U90 were made in DMSO yielding a final concentration of 1% DMSO in the assay. Data fitting was done using the GraFit 4 software.

Inhibition by Methanethiosulfonates in the Presence of 2164U90. CHO cells with stable expression of the human apical (ileal) sodium/bile acid transporter were grown to confluence in the Cytostar SPA plates, and the inactivation due to alkylation by 10 mM MTSET was detected as reduced accumulation of 50 μM ^{14}C-taurocholate in MHBSS/NaCl. The stock solution of the MTS reagent was made in distilled water immediately prior to the experiment. Cells were allowed to equilibrate with 20 μM 2164U90 in 1% DMSO for 5 min prior to adding the MTSET, and the cells were exposed to the reagent for 1 min. Subsequently, the monolayers were washed with 50 μL MHBSS/NaCl/1% DMSO/0.1% BSA (99% fat-free) and allowed to reequilibrate in the same medium for 10 min before adding the ^{14}C-taurocholate. The CHO cell line expressing the human ASBT was a kind gift of Dr Paul Dawson.

RESULTS

2164U90 Inhibition of Human and Mouse Apical Sodium/Bile Acid Cotransporters. Non-linear fitting of data from initial accumulation of 5−40 μM ^{14}C-taurocholate to the Michaelis−Menten equation:

$$v = V_m \times [S]/(K_m + [S])$$

as shown in Figure 2, panel A, yielded K_m values of 9.4 ± 1.2 and 13 ± 4.3 μM for the human and mouse ASBTs, respectively. All data points represent the mean value of six wells. The IC_{50}/K_i values for inhibition of the ASBTs were determined from measurements of initial uptake and/or steady-state levels at varying concentrations of [^{14}C]-taurocholate and 2164U90 (shown in Figure 2, panel B). IC_{50} values were calculated by fitting the data to the Michaelis−Menten equation, and the corresponding K_i values were determined by applying the Michaelis−Menten equation modified for competitive inhibition kinetics:

$$K_i = IC_{50}/([S]/K_m - 1)$$

As can be seen in Figure 2, panel B, the K_i values obtained for 2164U90 inhibition of taurocholate accumulation in the HEK293 cells were ~10 and 0.068 μM for the human and mouse transporters, respectively. This 150-fold difference in the K_i values is not due to any difference in substrate affinity between the two ASBTs as shown in Figure 2, panel A.

2164U90 Inhibition of Mouse−Human Hybrid ASBTs. Several chimeric transporters starting at the mouse ASBT N-terminus and ending with the human ASBT C-terminus were made to identify the possible regions responsible for the different K_i-values for 2164U90 inhibition. Figure 3, panel A, illustrates the composition of these hybrid transporters in the context of a nine transmembrane segment 2D model. Fusions between the two ASBTs are made downstream of putative transmembrane regions 1, 3, 5, and 7 in this model. All chimeras except for MH C2 demonstrated wild-type transport activity as determined from taurocholate accumulation in transiently transfected HEK293 cells. Figure 3, panel B, shows the effect of 2 μM 2164U90 on uptake of

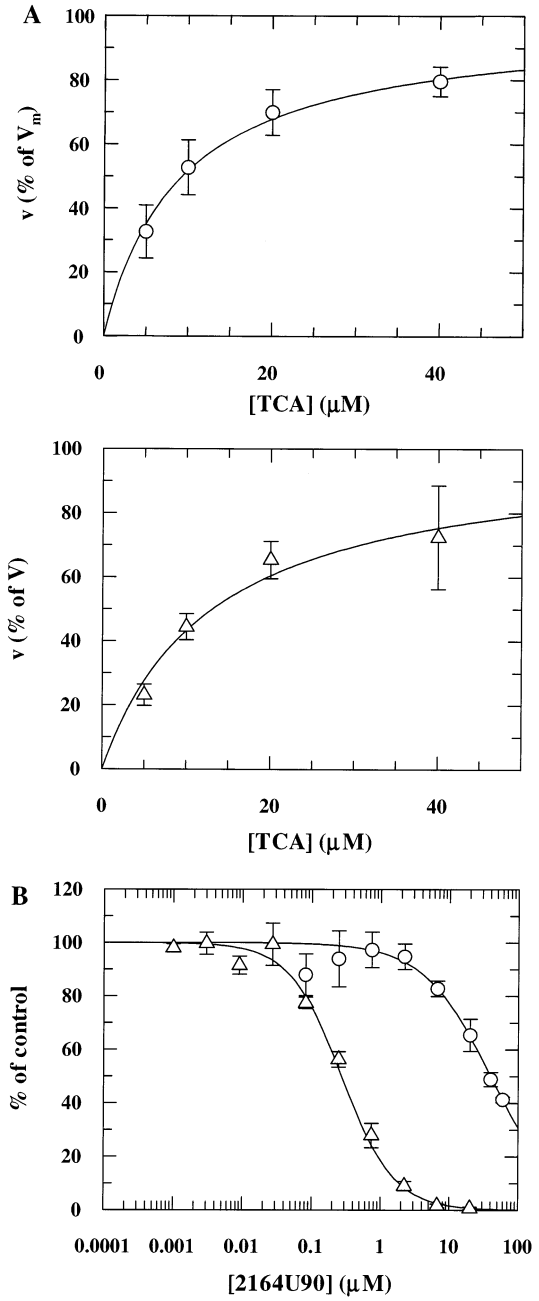

FIGURE 2: Kinetic constants for taurocholate transport and 2164U90 inhibition. (A) Apparent K_m values for taurocholate transport by the human (○) and mouse (△) apical sodium/bile acid cotransporters transiently expressed in HEK293 cells were determined at 20 °C in MHBSS containing 137 mM NaCl. Initial uptake rates for accumulation of the different concentrations of [^{14}C]-taurocholate (10 Ci/mol) were fitted to the Michaelis−Menten equation resulting in $K_{m,\ app}$ values of 9.4 and 13 μM for the human and mouse ASBTs, respectively (solid lines). (B) IC_{50} values for 2164U90 inhibition of the human (○) and mouse (△) ASBTs were established by monitoring the steady-state ($dt \sim 60$ min) accumulation of 50 μM ^{14}C-taurocholic acid at varying concentrations of 2164U90. Data were fitted to eq 2 (dose response, one site), and curves represent the best fits with IC_{50} values of 40 and 0.27 μM for the human and mouse ASBTs, respectively.

50 μM ^{14}C-taurocholate by the chimeras and wild-type transporters in the transfected cells. The inhibition seen in the accumulation of taurocholate is expressed as the percent of control (vehicle only) maximum. The ^{14}C-counts at steady-state accumulation were around 1000 CPM for the human ASBT and the mouse−human chimeras, whereas the mouse

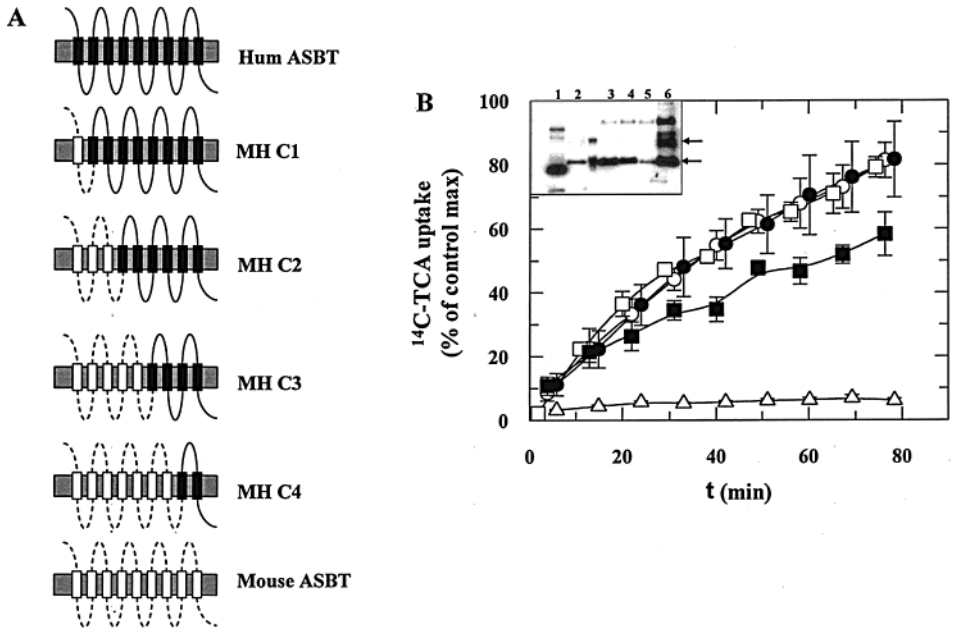

FIGURE 3: 2164U90 inhibition of mouse−human hybrid apical sodium/bile acid cotransporters. Chimeric ASBTs (panel A) were engineered and tested for 2164U90 sensitivity in transiently transfected HEK293 cells. Panel B shows uptake of 50 μM ^{14}C-taurocholic acid in the presence of 2 μM 2164U90 expressed as % of control maximum accumulation. The symbols used are (○) human ASBT, (●) MH C1, (□) MH C3, (■) MH C4, and (△) mouse ASBT. The inset displays a Western blot of total cell-lysates (~10 μg protein) from respective experiment with human ASBT (lane 1), MH C1 (lane 2), MH C2 (lane 3), MH C3 (lane 4), MH C4 (lane 5), and mouse ASBT (lane 6).

ASBT had a maximum taurocholate accumulation of ~3000 CPM at steady state (data not shown). Thus, 2 μM 2164U90 abolished most of the taurocholate uptake in the cells transfected with a construct encoding the mouse ASBT, while the mouse−human (MH) C1, C3, and C4 chimeras and the human ASBT all had higher, 60−80%, taurocholate accumulation in the presence of inhibitor. This result suggests that the residues or residues responsible for the different K_i values for the human and mouse ASBTs reside in the C-terminal part of the transporter. Western blots of total cell lysates from the Cytostar plates are shown as an inset in Figure 3, panel B, demonstrating that all constructs are well expressed mainly as a core glycosylated protein (marked by an arrow) in the SDS-PAGE analysis. The human ASBT has a somewhat lower molecular weight due to the single *N*-linked glycosylation site as compared to the chimeras and the mouse ASBT that all have two *N*-linked consensus sites on their *N*-termini. The mouse ASBT shows additional bands (marked by the upper arrow) corresponding to higher glycosylation, indicative of a more efficient plasma membrane trafficking of this transporter as compared to the human ASBT and the mouse−human ASBT hybrids. This finding is in agreement with the higher end points of taurocholate accumulation seen with the mouse ASBT. Although the MH C2 chimera protein is expressed and present in the HEK293 cells, no taurocholate uptake activity was found.

2164U90 Inhibition of Human−Mouse ASBT Chimeras. Two human−mouse hybrid transporters, HM C3 and HM C4, were made to confirm the finding that the region downstream of Trp252 is responsible for the divergent 2164U90 inhibition seen with the human and mouse ASBTs. These chimeras have a N-terminal region from the human ASBT and their C-terminal part from the mouse transporter. Figure 4, panel A, shows the two chimeras in a nine transmembrane domain model with the transporter fusions for HM C3 and C4 made downstream of putative transmembrane segments 5 and 7, respectively. Both HM C3 and C4 are fully active when expressed transiently in HEK293 cells, as seen in Figure 4B (lower panel), which shows the taurocholate accumulation at steady-state (60 min). Figure 4B (upper panel) demonstrates the effect of 2 μM 2164U90 on uptake of 50 μM ^{14}C-taurocholate in the HEK293 cells. Both chimeras exhibit the same high sensitivity toward the inhibitor as the mouse ASBT and have less than 10% taurocholate accumulation at steady-state. This experiment demonstrates that the C-terminal domain of the transporters, starting at Trp252, contained the amino acids responsible for the difference in sensitivity to 2164U90 seen between the two species.

The inset in Figure 4B (lower panel) shows the immunoblot from cells lysed after the taurocholate uptake measurements in the Cytostar plates. All constructs are well expressed in the HEK293 cells and contain core glycosylated as well as some higher glycosylation products (right side arrows). Lanes 1, 2, and 3 are from the human ASBT, HM C3, and HM C4, respectively, and lane 4 shows the mouse ASBT. Constructs containing the C-terminus from the mouse ASBT, HM C3, HM C4, and the mouse wild-type transporter all demonstrate higher steady-state accumulation of taurocholate as well as more of the protein processed to a complex glycosylation product as compared with the equally expressed human ASBT (left side arrow). Thus, the C-terminus of the mouse ASBT appears to contain a stronger plasma membrane trafficking signal than the human wild-type transporter when compared in the context of the HEK293 cells.

Identification of Residues Interacting with 2164U90. When the human and mouse ASBT sequences are aligned downstream of Trp252, six nonconserved amino acids are found (marked by arrows in Figure 5, panel A) and were therefore candidates responsible for the difference in 2164U90 inhibition. These residues in the mouse ASBT, Leu260, Ser279, Asp282, Leu285, Thr294, and Val295, were all mutated

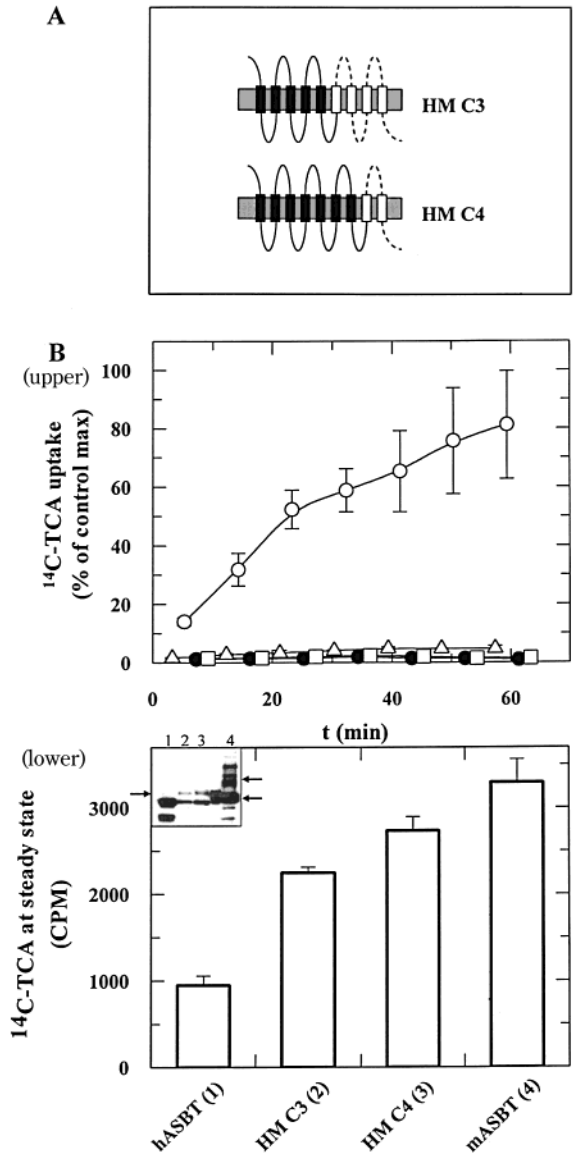

FIGURE 4: 2164U90 inhibition of human−mouse chimeras expressed in HEK293 cells. Hybrid transporters, HM C3 and HM C4 (panel A), encompassing N-terminal sequence from the human ASBT and ending with sequence from the mouse ASBT were tested for 2164U90 inhibition. The upper part of panel B shows the accumulation of 50 μM ^{14}C-taurocholic acid in the presence of 2 μM 2164U90 as the percent of control maximum at the end point. The human ASBT (○), HM C3 (●), HM C4 (□), and mouse ASBT (△) were all transiently expressed in HEK293 cells and the activity monitored in the Cytostar SPA plate. The lower part of panel B displays the control levels of ^{14}C-taurocholic acid at steady state, and the inset shows the Western blots of total cell-lysates from the corresponding experiments with human ASBT (1), HM C3 (2), HM C4 (3), and mouse ASBT (4).

individually or in combination to the corresponding amino acid(s) found in the human ASBT sequence. Figure 5, panel B, shows these positions (indicated by squares) in the context of the putative seven and nine transmembrane segment models (human ASBT sequence). It can be seen that only interaction between position 260 and 2164U90 would generate any topogenic information, as this residue is expected to be accessible only in the seven transmembrane 2D-model. The other residues are all likely to be partially or fully exposed in both putative 2D structures. Figure 6 (panel A) shows the steady-state levels (~60 min at room temperature) of ^{14}C-taurocholate accumulation in transiently transfected HEK293 cells. All wild-type and mutant SBATs transport taurocholate. Figure 6 (panel B) shows the uptake of 50 μM ^{14}C-taurocholate in the presence of 2 μM 2164U90 as the percent of control steady-state levels. The L260F, S279T, D282E, L285V, S279T/D282E, and S279T/D282E/L285V mutations in the mouse ASBT had no effect on the affinity of 2164U90 and all showed ^{14}C-taurocholate accumulation of around 10% or less in the presence of 2 μM 2164U90. Only data for the S279T mutant (filled squares) are shown along with trace for the mouse wild type ASBT (open triangles) in Figure 6, panel B, but all of these mutants displayed identical properties. In contrast, substitution of mouse ASBT Thr294 and Val295 with the corresponding human ASBT residues, Ser294 (filled triangle) and Ile295 (filled "inverted" triangle), resulted in a downward shift of the 2164U90 sensitivity. Individually substitutions of these amino acids appear to decrease the inhibition by 2 μM 2164U90 from about 90% seen with the mouse wild type ASBT to approximately 50%. In combination, substitutions of these two residues, Thr294 and Val295 to Ser294 and Ile295 fully "humanize" the mouse ASBT with respect to 2164U90 sensitivity (Figure 6, panel B, filled circles). As can be seen in Figure 5 (panel B), the position of residues 294 and 295 is exoplasmic in both 2D models.

Taurocholate Transport; $K_{m,app}$ Values for the Mouse ASBT T294S and T294S/V295I Mutants. The mouse ASBT mutants were expressed along with the wild-type transporter as described above. Figure 7 illustrates the uptake rate versus taurocholate concentration with the solid lines representing best fits to the Michaelis−Menten equation. The $K_{m,app}$ values were 9.3 ± 1.9, 27 ± 6.1, and 110 ± 49 μM for the mouse wild type and the mutants T294S/V295I and T294S ASBTs, respectively. The V_m values for the wild type and mutant transporters investigated depend directly on the fraction of the expressed protein that reaches the plasma membrane and vary between transfections and constructs as discussed above. Therefore, only the $K_{m,app}$ values are compared and used for analyzing the effect of amino acid substitutions in the mouse ASBT. The occupancy of positions 294 and 295 is outlined next to the graph displaying the saturation curves in Figure 7. It can be seen that removal of the one methyl group in the T294S mutant resulted in a 9-fold increase in the $K_{m,app}$. This increase in $K_{m,app}$ is reduced by adding the "missing" methyl group with the additional valine to isoleucine substitution in the T294S/V295I mutant. The substitution of T294 and V295 in the mouse ASBT to the corresponding residues serine and isoleucine residues of the human ASBT, S294, and I295 abolished the higher sensitivity due to 2164U90 inhibition seen in the mouse wild-type transporter as compared to the human ASBT.

Part of the binding interaction for this class of compounds as well as the bile acids can therefore be assigned to the most C-terminal exoplasmic surface of the transporters. In agreement with this hypothesis, this region has recently been demonstrated to be labeled by a 7-azido derivative of taurocholate (*24*).

2164U90 Inhibition of the Hamster and Rat Apical Sodium/Bile Acid Cotransporters. Figure 8, panel A, displays an alignment of the human, mouse, rat, and hamster ASBTs in the H8−H9 region. It can be seen that the hamster ASBT is identical with the mouse ASBT in positions 260, 279, 282,

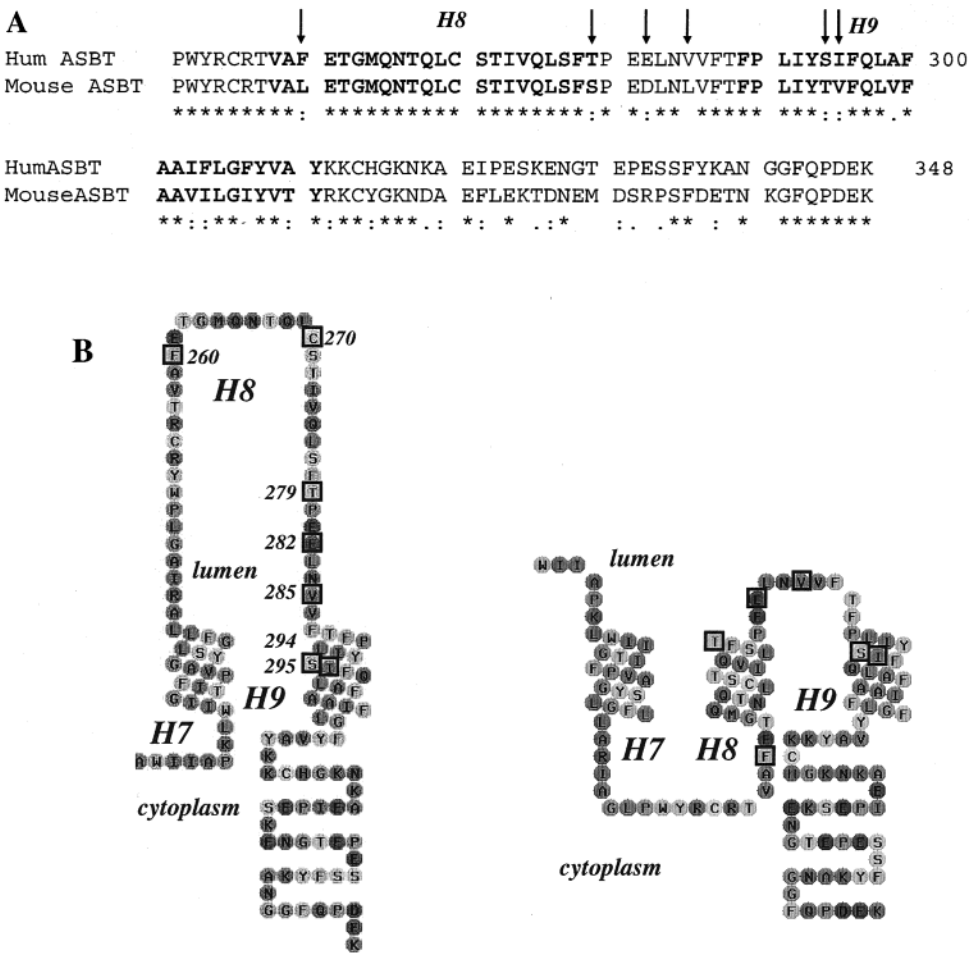

FIGURE 5: Alignment of the human and mouse ASBTs in the H8−H9 region. Arrows in panel A point to the nonconserved residues in the H8−H9 domain of the human and mouse ASBTs. Panel B shows the positions of the indicated residues in the context of the seven transmembrane (left side) and nine transmembrane (right side) 2D models for the sodium/bile acid cotransporters.

and 285 while it encompasses the same residues as the human ASBT in the 2164U90 sensitive positions 294 and 295. The rat transporter is identical with the mouse ASBT at all these positions. Thus, the hamster and rat ASBTs were expressed along with the human and mouse ASBTs in HEK293 cells, and the inhibition of accumulation of 50 μM ^{14}C-taurocholate by 2 μM 2164U90 was tested in the Cytostar 96 well plate. Figure 8 (panel B) shows the steady-state levels of ^{14}C-taurocholate as the percent of control and in the presence of the inhibitor. The hamster and human ASBTs both have ~90% remaining activity, as compared with the ~10% accumulation seen with the mouse ASBT in this experiment. In the same experiment, the rat ASBT demonstrates steady-state levels of ^{14}C-taurocholate at ~20% of the control accumulation. This finding provides further support for an important role of positions 294 and 295 in the interaction between the benzothiazepine 2164U90 and the apical sodium/bile acid cotransporters.

Irreversible Inhibition of the Human ASBT by a Side-Specific Thiophilic Methanethiosulfonate, MTSET; Protection of Target Cysteine 270 by 2164U90. Methanethiosulfonates are small-molecule thiol reagents that rapidly alkylate cysteines (*25*, *26*). The human apical and basolateral SBATs have been shown to be inactivated by the charged, exoplasmic specific methanethiosulfonates, MTSET and MTSES, at cysteine 270 and 266, respectively (*1*). This position is fully conserved among all known SBATs and the accessibility to MTS alkylation was demonstrated to be controlled by the natural substrates, sodium and bile acids (*23*). Here we have tested the ability of 2164U90 to protect the human ASBT from inhibition due to MTSET alkylation. CHO cells stably expressing the human transporter were preincubated with 20 μM 2164U90 with or without MTSET at 10 mM. Figure 9, left panel, shows the subsequent steady-state accumulation of 50 μM ^{14}C-taurocholate. The presence of 20 μM 2164U90 during the MTS reaction protects the transporter, resulting in ~70% remaining activity as compared with the ~40% activity observed with the control. This protective effect is concentration-dependent and is not detectable at 2164U90 concentrations below 1 μM (data not shown). This result suggests that 2164U90 is interacting not only with positions 294 and 295 but also has some overlap with position 270. Such an arrangement is not possible if cysteine 270 is placed as in the seven transmembrane model outlined in Figure 5B but, rather, favors a 2D-structure where putative H8 is a part of a binding pocket associated with the membrane domain. The bile acid competitive behavior of the inhibitor is also in agreement with the common site for substrate and 2164U90 with regards to protection from MTS alkylation.

DISCUSSION

The hypocholesteremic response from molecular intervention of the enterohepatic circulation at the level of intestinal

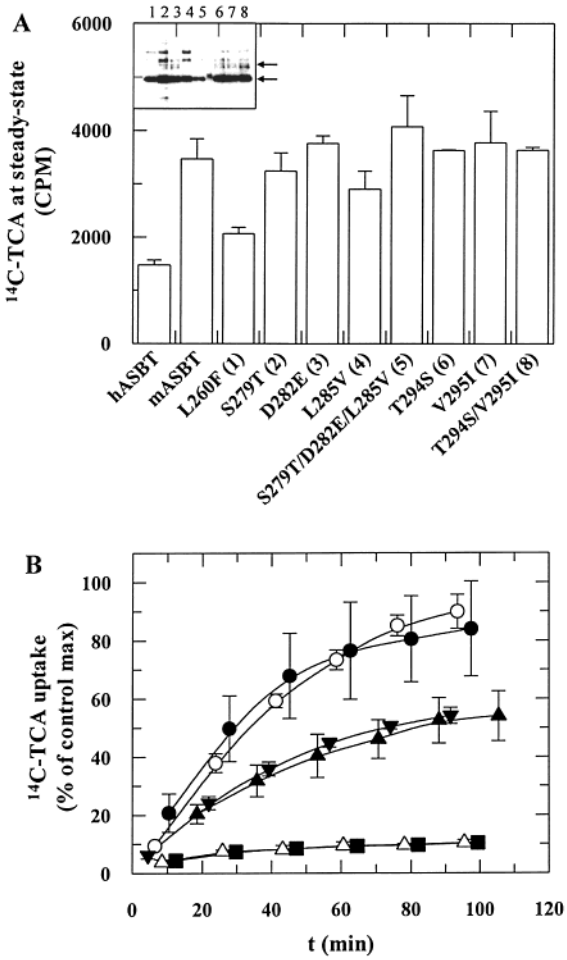

FIGURE 6: Site-directed mutagenesis in the mouse ASBT H8−H9 region: effect on 2164U90 sensitivity. Nonconserved residues in the mouse ASBT H8−H9 domain were substituted with the corresponding human ASBT residue either individually or in combinations. Panel A shows the steady-state levels (d$t \sim 60$ min) of accumulation of 50 μM ^{14}C-taurocholic acid for the various mouse ASBT mutants along with the wild type transporters, all transiently expressed in HEK293 cells. The inset displays a Western blot of the lysed cells (10 μg total protein) after the experiment with the lanes numbered in accordance to steady-state data. Panel B shows the uptake of 50 μM ^{14}C-taurocholic acid in the presence of 2 μM 2164U90 presented as the % of control maximum accumulation. The symbols used are (○) human ASBT, (●) mouse ASBT T294S/V295I, (▲) mouse ASBT T294S, (▼) mouse ASBT V295I, (■) mouse ASBT S279T, and (△) mouse ASBT.

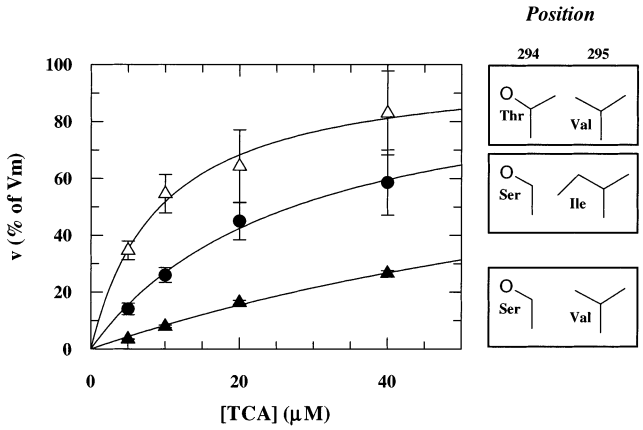

FIGURE 7: Kinetic constants for the mouse ASBT T294S and T294/V295I mutants. The $K_{m,app}$ values for taurocholic acid transport by the mouse ASBT T294S and T294S/V295I mutants were determined by measuring initial uptake of varying concentrations of ^{14}C-taurocholic acid in transiently transfected HEK293 cells. Accumulation of ^{14}C-taurocholic acid was followed for 10 min in the Cytostar SPA plate, with each data point representing the mean of six wells. Data were fitted to the Michaelis−Menten equation, and the curves represent the best fit with $K_{m,app}$ values of 9.3, 27, and 110 μM for the wild-type mouse ASBT, mouse T294S/V295I and T294S mutants, respectively. The left panel displays the corresponding amino acid configurations of positions 294 and 295.

bile acid reabsorption was first reported in the mid 1960s, when the bile acid sequestrant, cholestyramine, was introduced (*27*, *28*). Bile acid drainage as a concept for cholesterol lowering has been further strengthened since then; among the notable studies is the extensive POSH study where ileal bypass and cystectomy was proven to be a safe and effective way of lowering total as well as LDL cholesterol (*29*−*31*).

Candidate proteins involved in the flux of bile acid across the intestinal epithelium were initially identified by a photoaffinity strategy using photoreactive bile acid derivatives (*32*). In 1994, Dawson and co-workers used an expression cloning strategy to identify the sodium/bile acid cotransporter from hamster ileum and thereby set the scene for a rational investigation of transporter properties and bile acid transport inhibitors (*4*). A variety of bile acid reabsorption inhibitors with proven efficacy in both in vitro and in vivo models have been found (*18*, *19*, *21*, *22*). From such studies, a 3D QSAR pharmacophore model was created (*20*). The signature for a ligand recognized by the rabbit and human ileal transporters was shown to be the presence of a hydrogen bond donor, a hydrogen bond acceptor and three hydrophobic surfaces. Among the most potent inhibitors in the training set was a bile acid competitive benzothiazepine inhibitor structure, S0382 (2164U90), developed and reported by Burroughs Wellcome in 1995 (*21*, *22*).

Here, we demonstrate that conservative amino acid substitutions, Thr/Val to Ser/Ile, in the H8−H9 region of the mouse ASBT result in 150-fold decrease in sensitivity to 2164U90, the affinity seen with the human ASBT with only a small effect on the $K_{m,app}$ for the natural substrate. Substitution of only the threonine with a serine, however, also causes a significant shift in the substrate affinity, demonstrating the involvement of this position in the recognition of the bile acid as well.

A number of independent observations identifies the H8−H9 region as important for ligand recognition. Both bile acids and 2164U90 protect a fully conserved cysteine 270 (human ASBT sequence) in a highly preserved amphipathic region of the transporters from MTSET inactivation. Substitution of threonine 294 in the mouse ASBT to a serine causes a shift in both $K_{m,app}$ for taurocholate transport and the sensitivity to 2164U90 inhibition. In a recent investigation by Kramer and colleagues (*24*), it was demonstrated that a photoaffinity derivative of taurocholate labeled a 6−7 kDa C-terminal fragment starting in the center of the H8−H9 domain (between position 279 and 297 in the rabbit ASBT sequence). Thus, there is experimental support for a direct overlap between the binding sites for the bile acid and the competitive benzothiazepine class of inhibitor. Involvement of positions 294 and 295 in the interaction with 2164U90 is also supported by the finding that both the hamster and rabbit ASBTs, more homologous to the mouse ASBT in the H8−H9 region except for positions 294 and 295, where there is the serine/isoleucine substitution, have the same low 2164U90

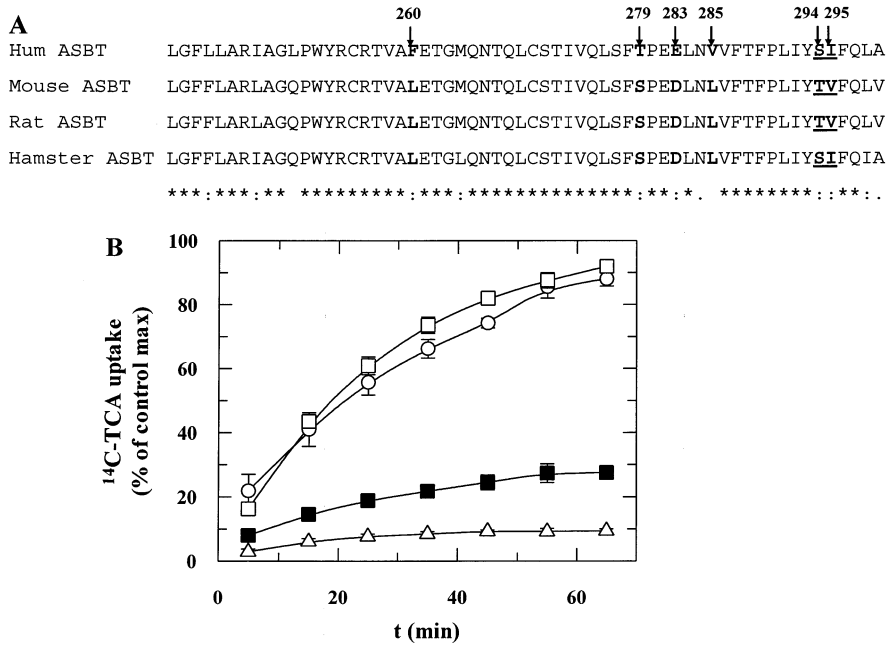

FIGURE 8: Species differences in the inhibition by 2164U90. Human, hamster, rat, and mouse apical sodium/bile acid cotransporters were all transiently expressed in HEK293 cells, and the uptake of 50 μM ^{14}C-taurocholic acid in the presence of 2 μM 2164U90 was recorded using the Cytostar SPA plate. Panel A shows the alignment of the H8−H9 region from the various species. Residues being nonconserved comparing the human and mouse ASBTs are indicated by arrows, and positions 294/295 are underlined. Inhibition by 2164U90 is displayed in panel B, where the symbols represent (○) human ASBT, (□) hamster ASBT, (■) rat ASBT, and (△) mouse ASBT.

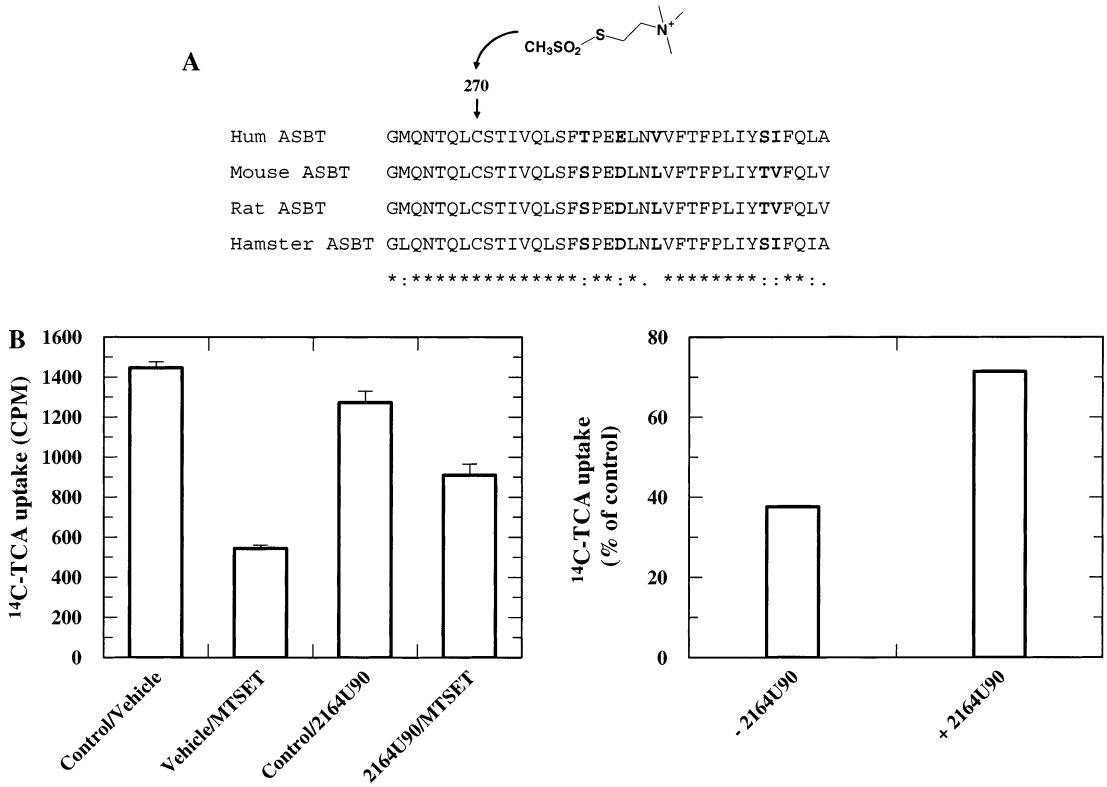

FIGURE 9: Inhibition due to MTS-alkylation; protection by 2164U90. CHO cells stably expressing the human apical sodium/bile acid cotransporter were preincubated with 20 μM 2164U90 before exposure to 10 mM MTSET for 1 min. Panel A displays the position of the target Cys270 in the context of the H8−H9 region. Levels of steady-state accumulation of 50 μM ^{14}C-taurocholic acid after exposure to MTSET in the presence or absence of 20 μM 2164U90 along with controls are shown in left part of panel B. The right panel gives the retained activities in percent of controls.

sensitivity as the human ASBT (Figure 8, (*20*)). The rat ASBT that is identical with the mouse transporter in the H8−H9 region has the same higher sensitivity toward 2164U90.

Several instances of polymorphism and mutations of the ileal bile salt transporter have been reported (*13*, *33*, *34*). Any polymorphism in positions 294 and 295 in this region could result in differing affinities for this class and perhaps other classes of bile acid transport inhibitors, although such polymorphism has not yet been found at the two residues that are critical for the differences in K_i reported here. If

these compounds come into clinical use, differences in response might enable the discovery of SNP's in this region.

The suggested location of cysteine 270 (human ASBT sequence) in the binding region for both bile acids and the bile acid competitive inhibitor, 2164U90, indicates proximity with positions 294 and 295. This is more in agreement with putative transmembrane H8 being at least membrane associated and not part of a long exoplasmic loop region (see Figure 5B). The amphipathic character and preservation of H8 makes it an attractive candidate for involvement in substrate binding and translocation. A recent investigation of the insertion properties of sequences in the human basolateral SBAT predicted to be transmembrane gave support for membrane association of all nine segments, including H8 (*15*).

Thus, the benzothiazepine, 2164U90, is a bile acid competitive inhibitor that interacts with the putative binding pocket for bile acids in the H8−H9 region of the apical sodium/bile acid cotransporters. These observations add to the evidence implicating this domain of the ileal bile acid transporter as being involved in ligand binding, namely, data that include including MTS inactivation (*1*), and photoaffinity labeling by the substrate (*24*).

ACKNOWLEDGMENT

We like to thank Dr. Jonas Boström for helpful discussions, Dr. Paul Dawson for the kind gift of the SBAT cDNAs and the CHO cells, and Dr. Olga Mareninova for technical assistance.

REFERENCES

1. Hallén, S., Fryklund, J., and Sachs, G. (2000) *Biochemistry 39*, 6743−50.
2. Kramer, W., and Wess, G. (1996) *Eur. J. Clin. Invest. 26*, 715−32.
3. Love, M. W., and Dawson, P. A. (1998) *Curr. Opin. Lipidol. 9*, 225−9.
4. Wong, M. H., Oelkers, P., Craddock, A. L., and Dawson, P. A. (1994) *J. Biol. Chem. 269*, 1340−7.
5. Christie, D. M., Dawson, P. A., Thevananther, S., and Shneider, B. L. (1996) *Am. J. Physiol. 271*, G377−85.
6. Hagenbuch, B., Stieger, B., Foguet, M., Lubbert, H., and Meier, P. J. (1991) *Proc. Natl. Acad. Sci. U.S.A. 88*, 10629−33.
7. GeneBank accession no. Z54357.
8. GeneBank accesion no. AJ131361.
9. Saeki, T., Matoba, K., Furukawa, H., Kirifuji, K., Kanamoto, R., and Iwami, K. (1999) *J. Biochem. (Tokyo) 125*, 846−51.
10. GeneBank accession no AB003303.
11. Wong, M. H., Oelkers, P., and Dawson, P. A. (1995) *J. Biol. Chem. 270*, 27228−34.
12. Hagenbuch, B., and Meier, P. J. (1994) *J. Clin. Invest. 93*, 1326−31.
13. Oelkers, P., Kirby, L. C., Heubi, J. E., and Dawson, P. A. (1997) *J. Clin. Invest. 99*, 1880−7.
14. Hallén, S., Brändén, M., Dawson, P. A., and Sachs, G. (1999) *Biochemistry 38*, 11379−88.
15. Hallén, S., Mareninova, O., Brändén, M., and Sachs, G. (2002) *Biochemistry 41*, 7253−66.
16. Kramer, W., Stengelin, S., Baringhaus, K. H., Enhsen, A., Heuer, H., Becker, W., Corsiero, D., Girbig, F., Noll, R., and Weyland, C. (1999) *J. Lipid Res. 40*, 1604−17.
17. Craddock, A. L., Love, M. W., Daniel, R. W., Kirby, L. C., Walters, H. C., Wong, M. H., and Dawson, P. A. (1998) *Am. J. Physiol. 274*, G157−69.
18. Wess, G., Kramer, W., Enhsen, A., Glombik, H., Baringhaus, K. H., Boger, G., Urmann, M., Bock, K., Kleine, H., Neckermann, G., and et al. (1994) *J. Med. Chem. 37*, 873−5.
19. Hara, S., Higaki, J., Higashino, K., Iwai, M., Takasu, N., Miyata, K., Tonda, K., Nagata, K., Goh, Y., and Mizui, T. (1997) *Life Sci. 60*, PL 365−70.
20. Baringhaus, K. H., Matter, H., Stengelin, S., and Kramer, W. (1999) *J. Lipid Res. 40*, 2158−68.
21. Root, C., Smith, C. D., Winegar, D. A., Brieaddy, L. E., and Lewis, M. C. (1995) *J. Lipid Res. 36*, 1106−15.
22. Lewis, M. C., Brieaddy, L. E., and Root, C. (1995) *J. Lipid Res. 36*, 1098−105.
23. Bonge, H., Hallen, S., Fryklund, J., and Sjostrom, J. E. (2000) *Anal. Biochem. 282*, 94−101.
24. Kramer, W., Girbig, F., Glombik, H., Corsiero, D., Stengelin, S., and Weyland, C. (2001) *J. Biol. Chem. 276*, 36020−7.
25. Smith, D. J., Maggio, E. T., and Kenyon, G. L. (1975) *Biochemistry 14*, 766−71.
26. Kenyon, G. L., and Bruice, T. W. (1977) *Methods Enzymol 47*, 407−30.
27. Whiteside, C. H., Fluckiger, H. B., and Sarett, H. P. (1966) *Proc. Soc. Exp. Biol. Med. 121*, 153−6.
28. Casdorph, H. R. (1967) *Vasc. Dis. 4*, 305−8.
29. Buchwald, H., Varco, R. L., Matts, J. P., Long, J. M., Fitch, L. L., Campbell, G. S., Pearce, M. B., Yellin, A. E., Edmiston, W. A., Smink, R. D., Jr., and et al. (1990) *N. Engl. J. Med. 323*, 946−55.
30. Buchwald, H., Campos, C. T., Boen, J. R., Nguyen, P. A., and Williams, S. E. (1995) *J. Am. Coll. Cardiol. 26*, 351−7.
31. Buchwald, H., Varco, R. L., Boen, J. R., Williams, S. E., Hansen, B. J., Campos, C. T., Campbell, G. S., Pearce, M. B., Yellin, A. E., Edmiston, W. A., Smink, R. D., Jr., and Sawin, H. S., Jr. (1998) *Arch. Intern. Med. 158*, 1253−61.
32. Kramer, W., Girbig, F., Gutjahr, U., Kowalewski, S., Jouvenal, K., Muller, G., Tripier, D., and Wess, G. (1993) *J. Biol. Chem. 268*, 18035−46.
33. Love, M. W., Craddock, A. L., Angelin, B., Brunzell, J. D., Duane, W. C., and Dawson, P. A. (2001) *Arterioscler. Thromb. Vasc. Biol. 21*, 2039−45.
34. Montagnani, M., Love, M. W., Rossel, P., Dawson, P. A., and Qvist, P. (2001) *Scand. J. Gastroenterol. 36*, 1077−80.

BI0205404